


Response of melt water and rainfall runoff to climate change and their roles in controlling streamflow changes of the two upstream basins over the Tibetan Plateau

Yueguan Zhang, Zhenchun Hao, Chong-Yu Xu  and Xide Lai

ABSTRACT

Located in the Tibetan Plateau, the upstream regions of the Mekong River (UM) and the Salween River (US) are very sensitive to climate change. The 'VIC-glacier' model, which links a degree-day glacier algorithm with variable infiltration capacity (VIC) model, was employed and the model parameters were calibrated on observed streamflow, glacier mass balance and MODIS snowcover data. Results indicate that: (1) glacier-melt runoff exhibits a significant increase in both areas by the Mann–Kendall test. Snowmelt runoff shows an increasing trend in the UM, while the US is characterized by a decreasing tendency. In the UM, the snowmelt runoff peak shifts from June in the baseline period 1964–1990 to May for both the 1990s and 2000s; (2) rainfall runoff was considered as the first dominant factor driving changes of river discharge, which could be responsible for over 84% in total runoff trend over the two regions. The glacial runoff illustrates the secondary influence on the total runoff tendency; (3) although the hydrological regime is rain dominated in these two basins, the glacier compensation effect in these regions is obvious, especially in dry years.

Key words | climate change, glacial runoff, snowmelt runoff, Tibetan Plateau, VIC-glacier model

Yueguan Zhang (corresponding author)
Xide Lai
Department of Water Conservancy and
Hydropower Engineering,
Xihua University,
Chengdu 610039,
China
E-mail: zhangyueguan@itpcas.ac.cn

Yueguan Zhang
Zhenchun Hao
State Key Laboratory of Hydrology-Water
Resources and Hydraulic Engineering,
Hohai University,
Nanjing 210098,
China

Chong-Yu Xu 
Department of Geosciences,
University of Oslo,
Oslo 0316,
Norway

INTRODUCTION

The Tibetan Plateau (TP) and the surrounding Himalayas, with an average altitude of 4,000 m a.s.l and an area of about 2.5×10^6 km², is the highest and most extensive highland and is also called the Third Pole (Qiu 2008). The TP exerts a profound influence on the East Asian and global climate (Lu *et al.* 2017), and is considered as a sensitive region and the amplifier for global climate change (Ma *et al.* 2006). The TP is also the source region of many major Asian rivers, such as the Brahmaputra, Mekong, Salween, Yellow and Yangtze Rivers, and is considered as the 'water towers of Asia' (Immerzeel *et al.* 2010; Zhang *et al.* 2013; Liu *et al.* 2018a). Discharge from these rivers sustains

the lives of hundreds of millions of people living downstream and so preservation of these water resources is crucial for social and economic development over these regions (Immerzeel *et al.* 2009; Liu *et al.* 2018a).

The TP is characterized by an abundance of glaciers and snow cover. The glacier area over the TP is about 91,822 km² (Kotlyakov *et al.* 2012) and is the third largest on Earth, after the Arctic/Greenland and Antarctic regions. Snow covers the majority of the TP during winter (Immerzeel *et al.* 2009). Glacier and snow cover over the TP is very sensitive to rising temperature. Studies based on observed meteorological data have suggested a warming trend over the TP in the past several decades, particularly since the 1980s (Duan & Wu 2006; Kuang & Jiao 2016), and the increasing rate is more rapid than that of surrounding areas (Wang 2017). Under the warming climate, the glaciers on the TP have generally been retreating, with the largest shrinkage in the

This is an Open Access article distributed under the terms of the Creative Commons Attribution Licence (CC BY-NC-ND 4.0), which permits copying and redistribution for non-commercial purposes with no derivatives, provided the original work is properly cited (<http://creativecommons.org/licenses/by-nc-nd/4.0/>).

doi: 10.2166/nh.2019.075

southeastern TP and the least in the interior and northwestern TP (Yao *et al.* 2004, 2012; Bolch *et al.* 2012). Simultaneously, snow coverage or snow water in the TP has also responded to climate change and experienced changes over the past period (Li *et al.* 2018). However, at present, there is no consistent conclusion about the snow cover change over the TP.

Glacier and snow are crucial water sources of rivers and greatly influence the hydrological and biological processes in the TP and the surrounding areas (Immerzeel *et al.* 2010; Kaser *et al.* 2010; Lutz *et al.* 2014; Chen *et al.* 2017; Li *et al.* 2018). The changes of glacier and snow cover due to the warming climate have exerted impacts on the water budgets over the TP (Liu *et al.* 2018a). In a warmer climate, snow will melt earlier in the year than it did before and likely affect the timing of runoff, especially in the spring when water demand for irrigation is high (Barnett *et al.* 2005). As well, changes in the amount of glacial runoff and precipitation also tend to greatly affect the volume of runoff over the TP (Yao *et al.* 2014). Yao *et al.* (2004) found that the glacial retreat in the 1990s has caused glacial meltwater runoff increasing by more than 5.5% in Northwestern China. The southeast TP, due to long-term perennial snow and glacier melting, has been shown to have among the highest total water storage depletion rates globally (Jacob *et al.* 2012; Yao *et al.* 2012; Chen *et al.* 2017).

In terms of river basin, Zhang *et al.* (2008) assessed the influence of glacier runoff and climate change on the river runoff over the Tuotuo river basin located in the source region of the Yangtze River, and indicated that a two-third increase in river runoff in the 1990s was caused by loss of ice mass as a result of warming climate. Also, Yao *et al.* (2014) have investigated the impacts of climate change and glacier on river runoff in the source region of the Yangtze River during 1986–2009, and found that the increased glacier-melt runoff due to temperature rising accounted for 17.5% of the total runoff changes and the remaining change was caused by the runoff induced from precipitation. In the Upper Brahmaputra River basin, the interannual variability of total water storage was controlled mainly by glacier mass changes driven primarily by temperature changes (Chen *et al.* 2017; Meng *et al.* 2019). In addition, the impact of climate change on water availability over the basins of Brahmaputra and Mekong Rivers was investigated by a hydrologic budget balance method, and the results indicate that increasing glacial meltwater had great effect on runoff changes during 1960–2010 (Liu *et al.* 2018b). Meanwhile,

in the upper Indus and Salween basin, it is found that the regional warming affected the local hydrology due to accelerated glacial melting during the simulation period (Immerzeel *et al.* 2009; Wang & Chen 2017). Furthermore, Cao *et al.* (2006) analysed the discharge change of five large rivers over the TP during the years 1956–2000, and found that climate change had a significant effect on the seasonal runoff variation, especially that in the spring. However, most of the above studies are based on statistical analysis of the observed data to characterize the controlling roles of melt water and rainfall runoff in the TP river flow change, and comprehensive quantitative investigations into attribution of streamflow trends to the different runoff components by hydrological simulation are still relatively few. In addition, few studies are involved in quantitative analysis of the response of rainfall runoff, glacial runoff and snowmelt to recent warming climate.

In this study, a degree-day glacier algorithm (Hock 2003) linking with the variable infiltration capacity (VIC) model (Liang *et al.* 1994), here referred to as VIC-glacier model (Zhang *et al.* 2013) was employed. The investigated areas are the upstream of the Mekong (UM) and Salween (US) rivers over the TP (Figure 1). The Mekong River and Salween River are important international rivers across China and Southeast Asia. Thus, runoff variation over these upper basins not only imposes great influence on local available water resources but also further affects water allocation in the middle and lower reaches. In addition, there are many large operating and planned hydropower stations along the trunks of both rivers, which are also very sensitive to the fluctuation of the upstream water resource induced by climate change. Based on gauge observations and the VIC-glacier model simulations, this work aims to: (1) investigate the long-term and decadal changes of rainfall runoff, snowmelt and glacial runoff in the two upstream basins during 1964–2013, in order to analyse the response of different runoff components to recent climate change; and (2) quantify the roles of the three runoff components in controlling river flow trends of the two basins in the past 50 years.

STUDY AREA AND DATA

Study area

In this study, the upstream regions of the Mekong River (UM) above Changdu station and the Salween River (US)

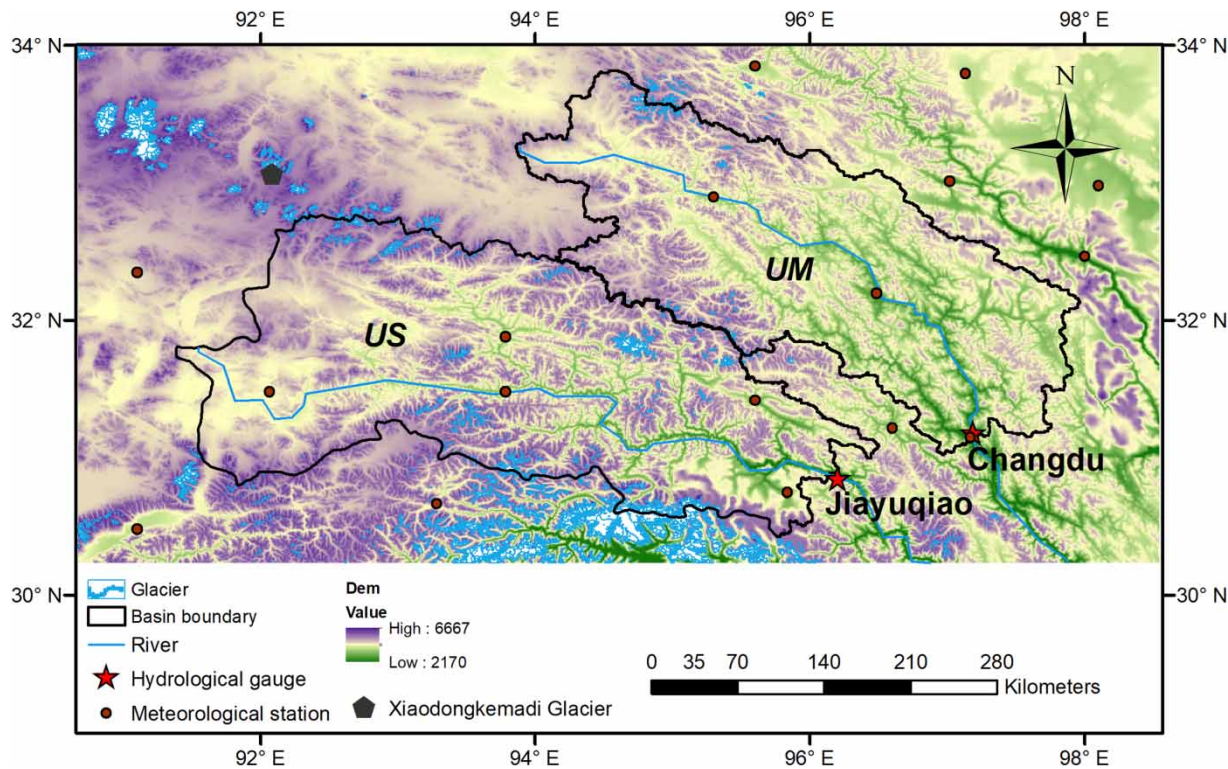


Figure 1 | Topography and boundary of the upstream of the Mekong river basin (UM) and the upstream of the Salween river basin (US) in the Tibetan Plateau.

above the Jiayuqiao hydrologic station were chosen as the study areas, respectively (Figure 1). The two upstream basins are located within 91–99°E and 30–34°N and cover a total area of about $1.21 \times 10^5 \text{ km}^2$ (Table 1). The elevation of the study basins varies from about 2,170 to 6,667 m a.s.l. The hydrological gauges of Changdu and Jiayuqiao are the control outlets of the UM and US, respectively (Figure 1). The UM and US are located in the southeastern TP and belong to the Tibetan Plateau climate system, characterized by a wet and warm summer and a cold and dry winter. The UM and US are predominantly affected by the monsoon in the summer (June–August) while in winter (December–February) westerlies

prevail. In addition, for the two regions, the US has the relatively large glacier coverage (about 1,152 km² and accounting for 1.7% of the basin area) whereas the UM has relatively less ice area (about 226 km² and 0.42% of the basin) (Table 1) (from the First Chinese Glacier Inventory: <http://westdc.westgis.ac.cn/glacier>).

Data

The atmospheric forcing data (maximum and minimum temperature, precipitation and wind speed), topography, soil and vegetation are required for running the VIC hydrological model. Other meteorological variables, such as

Table 1 | Characteristics of the two upstream basins

Basin	Gauge	Gauge location		Drainage area (km ²)	Glacier area (km ²)	Per cent of drainage area for glacier (%)
		Latitude (°)	Longitude (°)			
UM	Changdu	31.18	97.18	53,800	226.0	0.42
US	Jiayuqiao	30.85	96.20	67,740	1,151.6	1.7

vapour pressure, incoming shortwave radiation and net longwave radiation, can be calculated from daily temperature and precipitation (Kimball *et al.* 1997).

The daily meteorological data for the years 1964–2013 were collected from 17 stations of the National Climate Center of the China Meteorological Administration (CMA) in or around focus basins (Figure 1), and were fully quality controlled by CMA before releasing the data. All stations have records longer than 40 years, and 14 stations have continuous daily data spanning from January 1964 to December 2013. The dataset was created from *in-situ* observations applying solid quality control, including internal temporal and spatial consistency checks, homogeneity tests and potential outlier detection (Feng *et al.* 2004; Shen & Xiong 2016). The dataset was also regarded as the most credible meteorological dataset in China. All the station data were interpolated to the $1/12^\circ \times 1/12^\circ$ grids by using the inverse distance weighting (IDW) method. To account for temperature variations with elevation using the IDW method, monthly temperature lapse rates (Tlaps) or temperature gradients during 1964–2013 (Table 2) were derived by using linear regression analysis, i.e., fitting linear relationship between temperature and elevation of the weather stations. The correlation coefficient R for all months is more than 0.4, which indicates a good correlation between temperature and elevation, and meanwhile, the derived monthly temperature gradients can be applied properly in the IDW method.

Soil property data such as soil type, water-holding capacity and saturated hydrologic conductivity were obtained from the Food and Agriculture Organization (FAO) Soil Database, which provides the most detailed and globally consistent soil data (FAO 1988). The vegetation class and their parameters were derived from the University of Maryland's 1 km Global Land Cover product (<http://glcf.umd.edu/data/landcover/data.shtml>). Basic topography data over the study regions were obtained from GTOP30

(resolution: $1 \text{ km} \times 1 \text{ km}$) (http://eros.usgs.gov/#/Find_Data/Products_and_Data_Available/topo30_info).

Monthly observed streamflow data at Changdu (1964–2009) and Jiayuqiao (1980–1985) (Figure 1) were obtained from the Hydrological Bureau of the Ministry of Water Resource of China. These discharge records were used to evaluate the VIC-glacier model simulations in the two basins.

The initial glacier cover data over the UM and US were acquired from the First Chinese Glacier Inventory, which contains information about 26,000 glaciers throughout the whole country, and were digitized and archived by the 'Environmental and Ecological Science Data Center for West China' (<http://westdc.westgis.ac.cn/data/ff75d30a-ee7d-4610-a5a3-53c73964a237>). The glacier data were utilized to initialize the glacier percentage within each $1/12^\circ \times 1/12^\circ$ resolution grid. In addition, the glacier data from the Randolph Glacier Inventory 5.0 (<http://www.glims.org/RGI>) were used to assess the simulated glacier area changes between 1964 and 2013. Furthermore, observed glacier mass balance data for 1989–2012 at Xiaodongkemadi Glacier ($33^\circ 04' \text{N}$, $92^\circ 05' \text{E}$) (Figure 1) have been collected (Tong *et al.* 2016). The Xiaodongkemadi glacier is near the northern part of the upstream region of the Salween River (Figure 1). It has a total area of 1.8 km^2 , a length of about 2.8 km, and altitude elevation ranging between 5,380 m and 5,926 m.

In addition, the global 8-day and 0.05° Moderate Resolution Imaging Spectroradiometer (MODIS) snow products (MOD10C2) (<http://nsidc.org/data/modis/index.html>) during 2001–2013 were used for snow cover analysis over the two upstream basins. Previous assessments over the TP have revealed that the MODIS snow product generally has sufficient accuracy to reflect snow cover information over the TP (Pu *et al.* 2007; Li *et al.* 2018). These studies have also suggested that the MODIS data can be used to assess the snow cover dynamics in the TP.

Table 2 | Monthly temperature lapse rate (Tlaps) ($^\circ \text{C}/\text{km}$) and correlation coefficient (R) between temperature and elevation

Month	Jan	Feb	Mar	Apr	May	Jun	Jul	Aug	Sep	Oct	Nov	Dec
Tlaps	−3.8	−4.1	−4.4	−4.6	−4.5	−3.8	−3.9	−3.9	−3.5	−3.9	−4.2	−3.8
R	0.45	0.51	0.57	0.73	0.75	0.70	0.79	0.79	0.66	0.62	0.55	0.47

METHOD

Hydrological model

In this study, the VIC model (Liang *et al.* 1994, 1996) was employed. The VIC model is a grid-based land surface scheme which parameterizes the dominant hydrometeorological processes taking place at the land surface-atmosphere interface. The model is characterized by a mosaic representation of land surface cover and a subgrid parameterization for infiltration, which accounts for sub-grid scale heterogeneities in land surface hydrologic processes (Su *et al.* 2005). The soil column comprises three soil layers, which allows the representation of the rapid dynamics of soil moisture movement during storm events and the slower deep inter-storm response in the bottom layer. Three types of evaporation are considered in the model. They are evaporation from the canopy layer of each vegetation class, transpiration from each of the vegetation classes and evaporation from bare soil. Total evaporation over the grid cell is computed as the sum of the three individual evaporation elements (Liang *et al.* 1994). For details of each part related to water balance and energy fluxes, please refer to the investigation by Liang *et al.* (1994).

However, there is no incorporation of a glacier melt module in the current official version of the VIC model to simulate melting processes for icebergs in the glaciated mountainous regions. Recently, a 'VIC-glacier' model which links a simple degree-day glacier algorithm with the original VIC model has been developed to do hydrological modelling over basins with glacier in the TP (Zhang *et al.* 2013). In this study, we utilized this VIC-glacier model. The total runoff includes the glacier meltwater from each grid which is estimated as:

$$R(i) = f \times M_i + (1 - f) \times R_{vic} \quad (1)$$

where $R(i)$ is the total runoff (mm) in grid i ; f is the ratio of glacier area over grid i ; R_{vic} is the estimated runoff for the ice-free part in grid i ; M_i is the calculated melt runoff (mm) from the glacier part in grid i using the degree-day model.

The glacier volume is estimated using a modified equation:

$$V = 0.04 S^{1.43} \quad (2)$$

where V is the ice volume and S is the total glacier area. The initial ice volume in the catchment was estimated from an inversion of Equation (2) using glacier surface area derived from the glacier distribution data. In our study, the VIC-glacier model was set up over the study basins at a spatial resolution of $1/12^\circ \times 1/12^\circ$.

Model parameters

The performances of the VIC-glacier model in the UM and US largely rely on two categories of model parameters: (1) degree-day factors (DDFs) for simulating meltwater over glacierized areas, including degree-day factors for snow (DDF_{snow}) and ice (DDF_{ice}); and (2) parameters in the VIC model for simulating runoff in non-glacierized areas. In this study, the initial values of degree-day factors for snow (DDF_{snow}) and ice (DDF_{ice}) in the UM and US were determined from the investigated results of Zhang *et al.* (2006), which indicated an average DDF_{snow} of $4.1 \text{ mm } ^\circ\text{C}^{-1} \text{ day}^{-1}$ and DDF_{ice} of $7.1 \text{ mm } ^\circ\text{C}^{-1} \text{ day}^{-1}$ for western China based on glacier mass balance observations. Then, the glacier area changes between the first China Glacier Inventory and Randolph Glacier Inventory 5.0, and the observed monthly flows for the two upstream basins, were utilized to calibrate the degree-day factors. The final adopted values of the DDF_{snow} and DDF_{ice} for the two basins are listed in Table 3.

The parameters of the VIC model needing calibration include the infiltration parameter (b_{inf}), the depth of the first and second soil layers (D_1 and D_2), and the three base flow parameters (Ws , D_{max} and D_s) (Su *et al.* 2005). The parameter b_{inf} , which has a common range of 0–0.4, defines the shape of the VIC curve. The first soil depth (D_1) for each grid was set to 5–10 cm, according to the investigation of Liang *et al.* (1996). The three base flow parameters, which affect the flow and storage of the water in the third layer, generally need minor adjustment during the calibration. Hence, only the infiltration-shape

Table 3 | Values of parameters adopted in the VIC model

Parameter	Description	Range	UM	US
DDF _{ice} (mm °C ⁻¹ day ⁻¹)	Degree-day factor for ice-melt	3.4–13.8	11.5	7.1
DDF _{snow} (mm °C ⁻¹ day ⁻¹)	Degree-day factor for snowmelt	3.0–7.9	6.5	4.1
D _s (fraction)	Fraction of D _{smax} where non-linear baseflow begins	0–1	0.03	0.02
D _{smax} (mm/d)	Maximum velocity of baseflow	0–50	10	10
W _s (fraction)	Fraction of maximum soil moisture where non-linear baseflow occurs	0–1	0.9	0.9
b _{inf}	Variable infiltration curve parameter	0–0.4	0.3	0.2
D ₂ (m)	Thickness of the second soil moisture layer	0–3	1.5	1

parameter (b_{inf}) and the second layer depth (D₂) were targeted for intensive calibration (Table 3). The range of these parameters refers to previous studies (Kayastha et al. 2003; Su et al. 2005).

In this study, the manual calibration process, i.e., the trial and error method, was employed to calibrate DDFs and the VIC model to improve its hydrological performance in the two upstream regions over the TP. The percent bias (PBIAS) and Nash–Sutcliffe efficiency coefficient (NSE) were used as the VIC evaluation statistics during the model calibration. PBIAS and NSE are defined as follows:

$$NSE = 1 - \frac{\sum_{i=1}^n (Y_i^{obs} - Y_i^{sim})^2}{\sum_{i=1}^n (Y_i^{obs} - Y^{mean})^2} \quad (3)$$

$$PBIAS = \frac{\sum_{i=1}^n (Y_i^{sim} - Y_i^{obs}) * 100}{\sum_{i=1}^n (Y_i^{obs})} \quad (4)$$

where Y_i^{obs} and Y_i^{sim} are the observed data and simulated value at time i ; Y^{mean} is the mean of observed data for the whole evaluating period. The final calibrated parameters used in the VIC-glacier model are shown in Table 3.

Trends and attribution analyses

In this study, the Mann–Kendall test (Mann 1945; Kendall 1975) was used to examine the monotonic trend of hydrometeorological variables for the period of 1964–2013. In this

method, the standard normal statistic Z is estimated by:

$$Z = \begin{cases} (S - 1) / \sqrt{\text{Var}(S)} & \text{if } S > 0 \\ 0 & \text{if } S = 0 \\ (S + 1) / \sqrt{\text{Var}(S)} & \text{if } S < 0 \end{cases} \quad (5)$$

$$S = \sum_{i=1}^{n-1} \sum_{j=i+1}^n \text{sgn}(x_j - x_i) \quad (6)$$

$$\text{sgn}(\theta) = \begin{cases} 1 & \text{if } \theta > 0 \\ 0 & \text{if } \theta = 0 \\ -1 & \text{if } \theta < 0 \end{cases} \quad (7)$$

$$\text{Var}(S) = \left[n(n-1)(2n+5) - \sum_t t(t-1)(2t+5) \right] / 18 \quad (8)$$

where t is the extent of any given tie. A positive value of Z indicates an increasing trend and vice versa. The test statistic Z is not statistically significant if $-Z_{\alpha/2} < Z < Z_{\alpha/2}$ while it is statistically significant if $Z < -Z_{\alpha/2}$ or $Z > Z_{\alpha/2}$.

In order to quantify the trend magnitude, the Theil–Sen approach (TSA) was employed (Kumar et al. 2009). The TSA slope β is defined as:

$$\beta = \text{Median} \left(\frac{x_j - x_i}{j - i} \right) \quad \text{where } 1 < i < j < n \quad (9)$$

Positive and negative β values indicate an increasing or decreasing trend, respectively.

In this study, total runoff consists of rainfall runoff, snowmelt and glacial runoff. Thus, a change in individual runoff component will cause variation of the total runoff, and vice versa. The trend for total runoff is the sum of the trends of the three individual runoff

components. Such changes can be described by the following formula:

$$\Delta R = \Delta R_r + \Delta R_s + \Delta R_g \quad (10)$$

where ΔR is the trend in total runoff for 1964–2013, ΔR_r , ΔR_s and ΔR_g are the trend for rainfall runoff, snowmelt and glacial runoff over the same period, respectively. The trend magnitude for total runoff (ΔR), rainfall runoff (ΔR_r), snowmelt runoff (ΔR_s) and glacial runoff (ΔR_g) can be calculated by Equation (9). Furthermore, the per cent contribution of trend in individual runoff variable to the tendency of the total runoff can be calculated as follows:

$$P_r = \frac{\Delta R_r}{\Delta R} * 100, \quad P_s = \frac{\Delta R_s}{\Delta R} * 100, \quad P_g = \frac{\Delta R_g}{\Delta R} * 100 \quad (11)$$

where P_r , P_s and P_g are percentage contributions of the trend in the rainfall runoff, snowmelt runoff and glacial runoff to the total runoff trend, respectively. This can be regarded as an attributing method which quantitatively describes the controlling role of the individual runoff element in the total runoff trend. The sum of per cent contributions for the three runoff constituents should equal 100%. The method utilizing per cent contribution to quantify the role of hydrological component in the change of some environmental variables has been widely employed in hydrological researches (Wu *et al.* 2014; Yao *et al.* 2014; Meng *et al.* 2019).

RESULTS

Model validation

Figures 2 and 3 provide the observed and VIC-glacier model simulated monthly time series of hydrograph for the UM (1964–2009) and US basins (1980–1985). Also, comparisons between mean monthly modelled and measured hydrograph are presented in Figure 4. Table 3 lists calibrated values for the chosen parameters in each focus region, which were determined by using trial and error techniques. In addition,

the deriving evaluated statistics for the modelling efficiency over the two regions are shown in Table 4.

Generally, the simulated monthly streamflow during the focus period can capture the observed evolution and magnitude reasonably for the two upstream basins, with NSE of 0.73 and 0.86 for the UM and US, respectively (Figures 2 and 3). From Figures 2 and 3, it can be distinguished that the simulated baseflow of the VIC-glacier model is less than the observed flow. One plausible reason is due to seasonal frozen soil over the two basins which would negatively affect the VIC baseflow simulation to some extent. However, the major hydrologic characteristics, such as the timing and amplitude of the discharge peaks, the rising and recessing limb of hydrograph (Figure 4), the modelling result for the UM and US, can basically reproduce the pattern of observed flow, which further validates the good efficiency of the VIC-glacier model in terms of the streamflow simulation.

Figure 5(a) and 5(b) compare the VIC simulated and MODIS estimated mean monthly snow cover extent (fraction of basin area with snow). For both regions, the VIC model underestimates snow cover extent during all months in comparison with MODIS estimation. However, in respect of the pattern of snow dynamics related to the timing of snow accumulation and snow depletion, there is a good consistency between the VIC simulation and MODIS output, i.e., snow beginning to form accumulations around late September and starting to melt about early March for both the VIC modelling results and remote sensing estimate outcomes. Simultaneously it can be found, for any month, the difference between the VIC simulated snow cover and estimation from MODIS is no more than 15% in the UM and US. Also, with regard to modelling snow cover change, it can be understood that both the outcomes from VIC simulation and MODIS estimation contain large uncertainties (Cuo *et al.* 2013; Chen *et al.* 2017). In addition, because of the scarcity of observed data and some unpredictable processes (such as snow drift), snow melting is too complicated to fully represent, which may be the reason for underestimation of snow cover. Thus, on the whole, it can be identified that VIC modelling results can basically reflect the seasonal cycles of the satellite estimations.

Furthermore, with regard to the degree-day model in simulating glacier melt, Figure 6 illustrates the observed

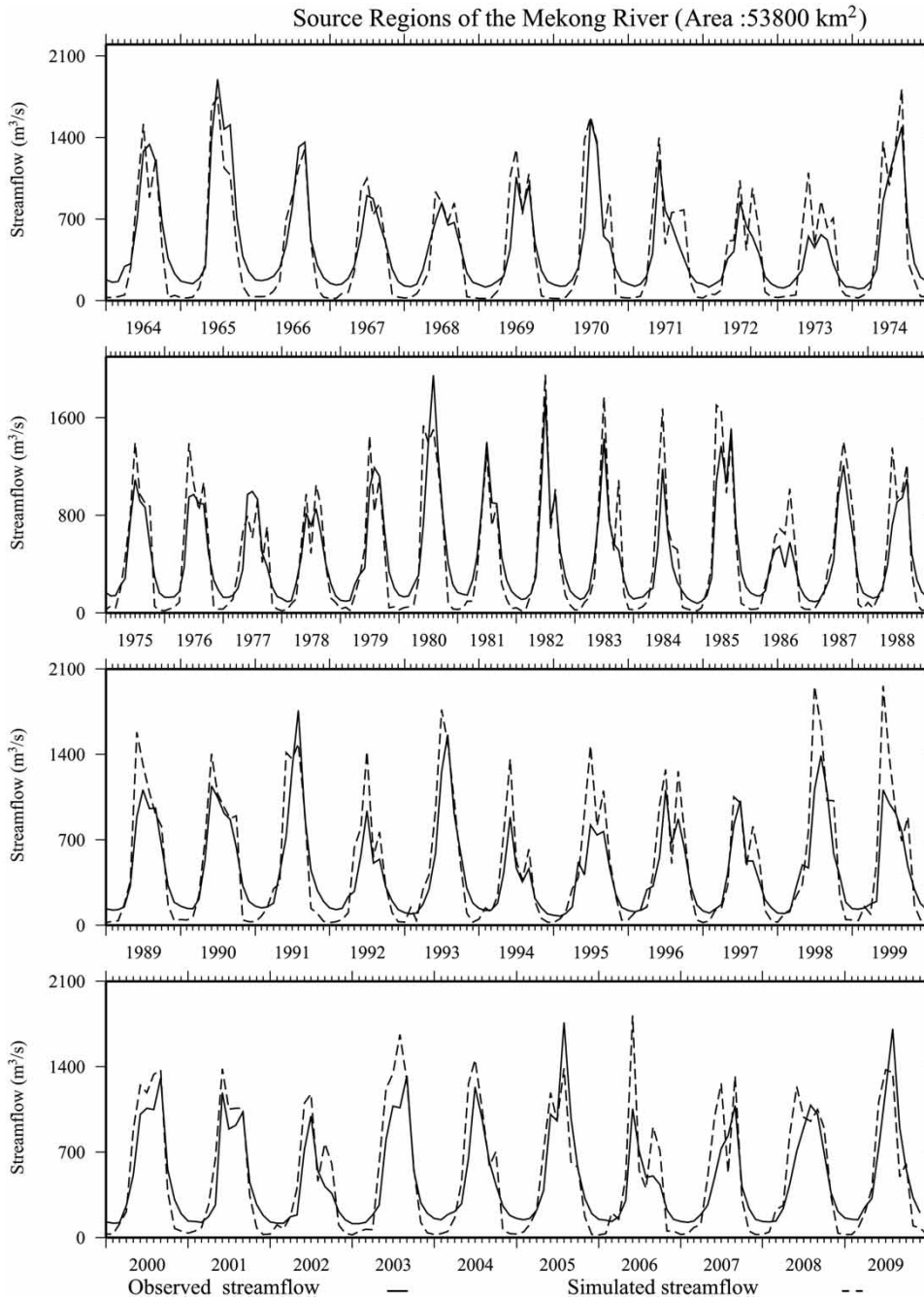


Figure 2 | Observed and modelled monthly streamflow for the upstream region of the Mekong River basin at Changdu gauge for 1964–2009.

and simulated annual mass balance of Xiaodongkemadi Glacier for 1989–2012 with a correlation coefficient of 0.81 and relative bias of -1.31% . Meanwhile, from the statistical results, the VIC-glacier model simulated a decrease in glacier areas of -26.0% in the UM and -22.0% in the US

during 1968–2010, which are generally close to the observed changes of -29.0% and -20.0% in the two basins between the first Chinese Glacier Inventory and the Randolph Glacier Inventory 5.0 data, respectively. Thus, the good consistency between simulated results and measured data

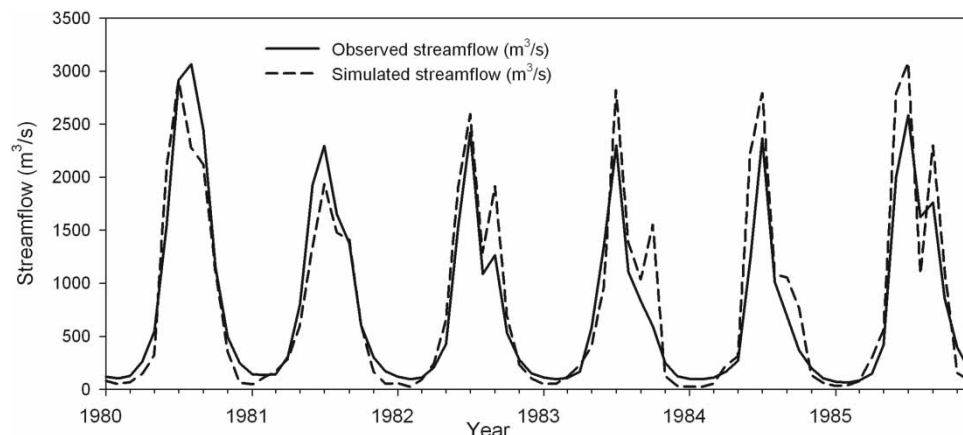


Figure 3 | Observed and modelled monthly streamflow for the upstream region of the Salween River basin at Jiayuqiao gauge for 1980–1985.

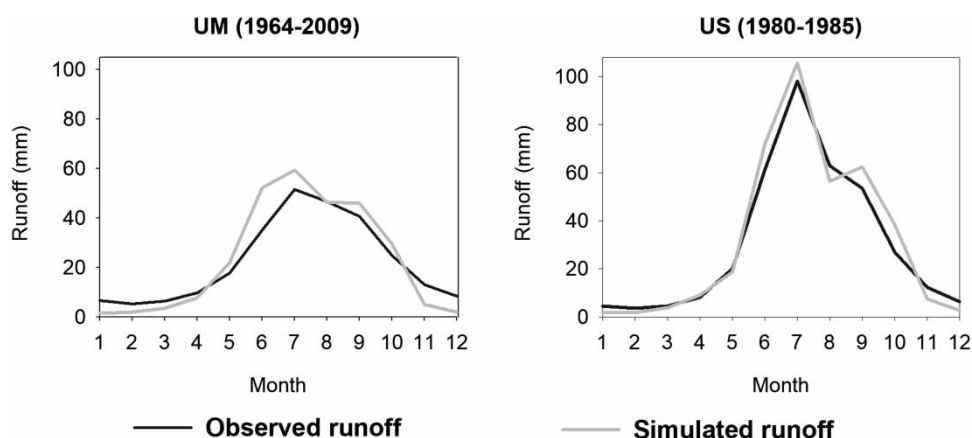


Figure 4 | Mean monthly observed and VIC simulated total runoff for the UM and US over respective period with measured flow.

Table 4 | Nash–Sutcliffe efficiency (NSE) and percent bias (PBIAS) of the simulated monthly streamflow relative to the observations for the UM (1964–2009) and US (1980–1985)

Basin	Observed annual runoff (mm)	Simulated annual runoff (mm)	NSE	PBIAS (%)
UM	278.35	279.60	0.73	0.45
US	361.95	380.26	0.86	5.1

suggests the feasibility of the VIC-glacier model in modelling glacier runoff in the study regions.

On the whole, the VIC-glacier model can reproduce the evolution and magnitude of the observed streamflow at the UM and US; the VIC performance in simulating snow cover shows acceptable results; and the modelling glacier

annual mass balance and glacier area change are comparable to the observed data.

Runoff components

In this study, the total runoff consists of three components: rainfall runoff (including direct rainfall surface runoff and sub-surface runoff), snowmelt runoff (surface runoff from melting snow) and glacier runoff (runoff from melting ice on the glaciated area). [Figure 7](#) presents the seasonal distribution of the runoff components, and [Table 5](#) gives their corresponding per cent contribution to the total annual runoff for the UM and US basins during the period of 1964–2013.

The rainfall runoff contributes to a respective 85.66% and 85.81% of total runoff for the UM and US ([Table 5](#)).

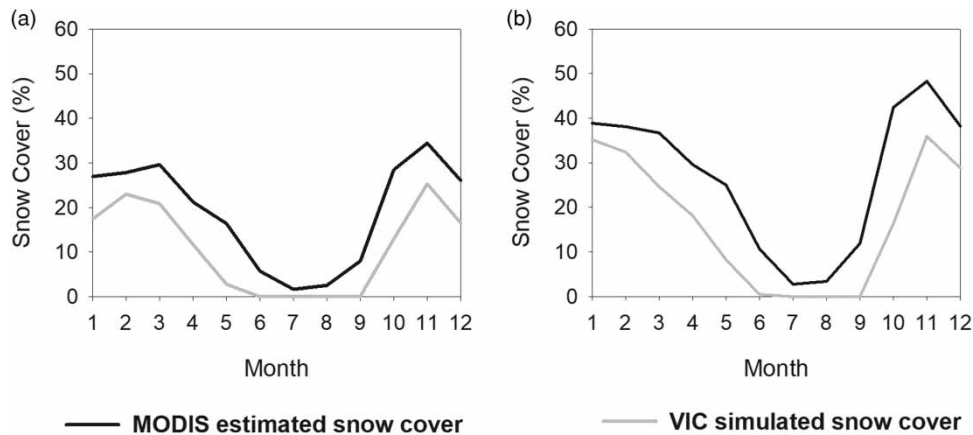


Figure 5 | Long-term mean monthly MODIS estimated snow cover versus VIC simulated snow cover during 2001–2013: (a) results for the UM; (b) results for the US.

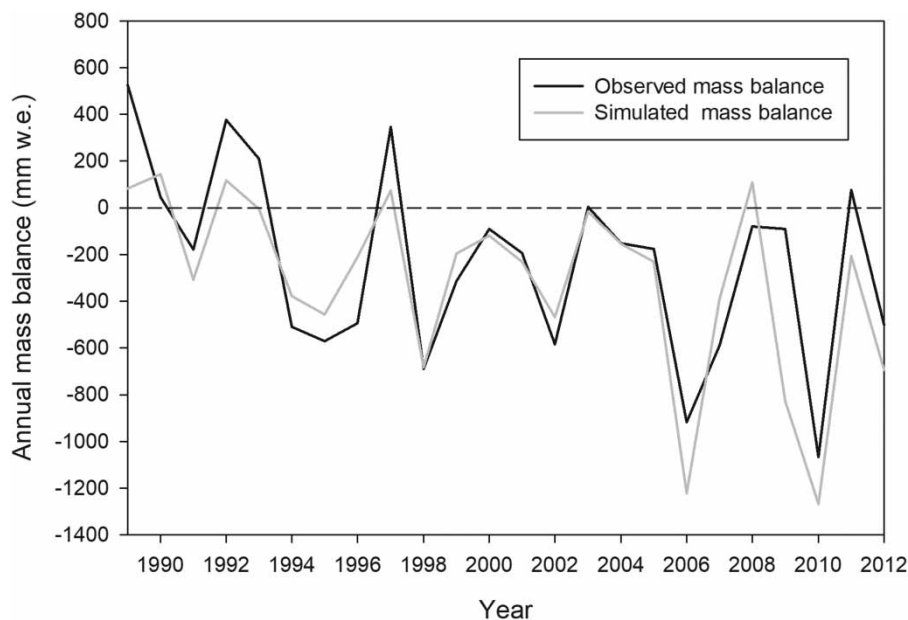


Figure 6 | Observed and simulated annual mass balance of the Xiaodongkemadi Glacier for the years 1989–2012.

This suggests that the monsoon rainfall plays an important role in the runoff generated in the two regions. The snowmelt water, which contributes about 12.37% and 6.87% of the annual total runoff in the UM and US, is an important water source especially for irrigation in the spring season. It can be identified from [Figure 7](#) that there are two peaks in the mean monthly snowmelt runoff over the focus basins, with one in June and the other in October. The snowmelt in spring or early summer, which is from the

accumulated snowpack in winter and the snow falling in spring, mostly occurs during April–June and reaches the peak in June along with the rise of temperature. With regard to the snowmelt peak in the October, it is probably ascribable to the fresh snowfall in September and October, which melts immediately after a short stay of a few days above the ground. There are similar phenomena in other regions such as the Kaidu River in northwestern China ([Shen *et al.* 2018](#)). The contribution of the glacier runoff to

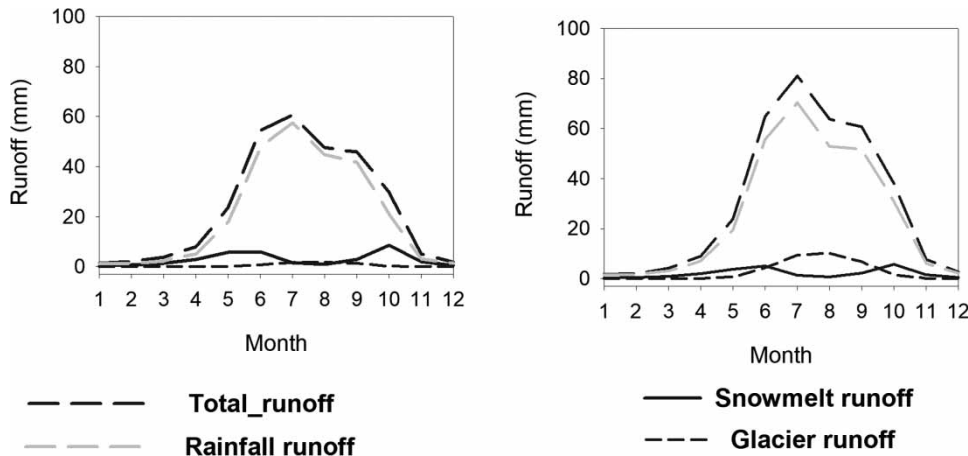


Figure 7 | Mean monthly VIC simulated total runoff and three runoff components for the UM and US during 1964–2013.

Table 5 | Contribution of simulated glacier runoff, snowmelt and rainfall runoff to total runoff during 1964–2013

Basin	Total runoff	From glacier melt (%)	From snowmelt (%)	From rainfall runoff (%)
UM	278.35 mm	1.97	12.37	85.66
US	362.00 mm	7.32	6.87	85.81

total runoff differs between the two basins, with a proportion about 1.97% over the UM and a larger ratio (7.32%) in the US, respectively (Table 5).

Changes for rainfall runoff, snowmelt, glacier-melt runoff and total runoff

Generally, annual temperature and precipitation across the two upstream basins indicate an overall increasing trend during the years 1964–2013. Both annual precipitation and temperature in the UM indicate a statistically increasing trend, at α 0.05 significance level by using Mann–Kendall test. The US is similar to the UM except for precipitation being a non-significant up trend. Figure 8 further demonstrates mean monthly precipitation and temperature for the two upstream basins over three time slices to further reveal decadal climate change occurred in the past 50 years. Under climate change, the rainfall runoff, snowmelt and glacier runoff have experienced corresponding changes.

The linear trends for annual simulated rainfall runoff, snowmelt and glacier-melt runoff for the past 50 years

were derived (Table 6). Rainfall runoff generally indicates an overall increasing trend from 1964 to 2013 in both regions, of which it is significant at α 0.05 significance level in the UM by the MK test. Meanwhile, the modelling glacier-melt runoff exhibits a significant increase in both areas by the MK test. However, simulated snowmelt shows non-significant increasing trend in the UM while the US is characterized by a decreasing tendency. The total runoff in the UM displays a significant increase during 1964–2013.

To evaluate potential changes in runoff-generated regimes, we separated our results into three periods, i.e., 1964–1990 (baseline period), 1991–2000 (1990s) and 2001–2013 (2000s). Figure 9 illustrates mean monthly rainfall runoff, snowmelt, glacial runoff and total runoff for the three periods in the study basins.

Figure 9(a) and 9(b) show results of long-term average monthly rainfall runoff in three periods. In the UM, compared to the baseline period of 1964–1990, increasing rainfall runoff can be found in nearly all months for both the 1990s and 2000s, with a respective increment of 10% and 12% during the two periods. In the US, the rainfall runoff in June and August in the 1990s shows some decreases while July indicates a little increase, and the final statistical analysis suggests a slight reduction over the 1990s relative to the baseline period. However, during the 2000s, moderate increase can be observed in the warm season (April to September except for July and August) in the US and, therefore, the annual mean

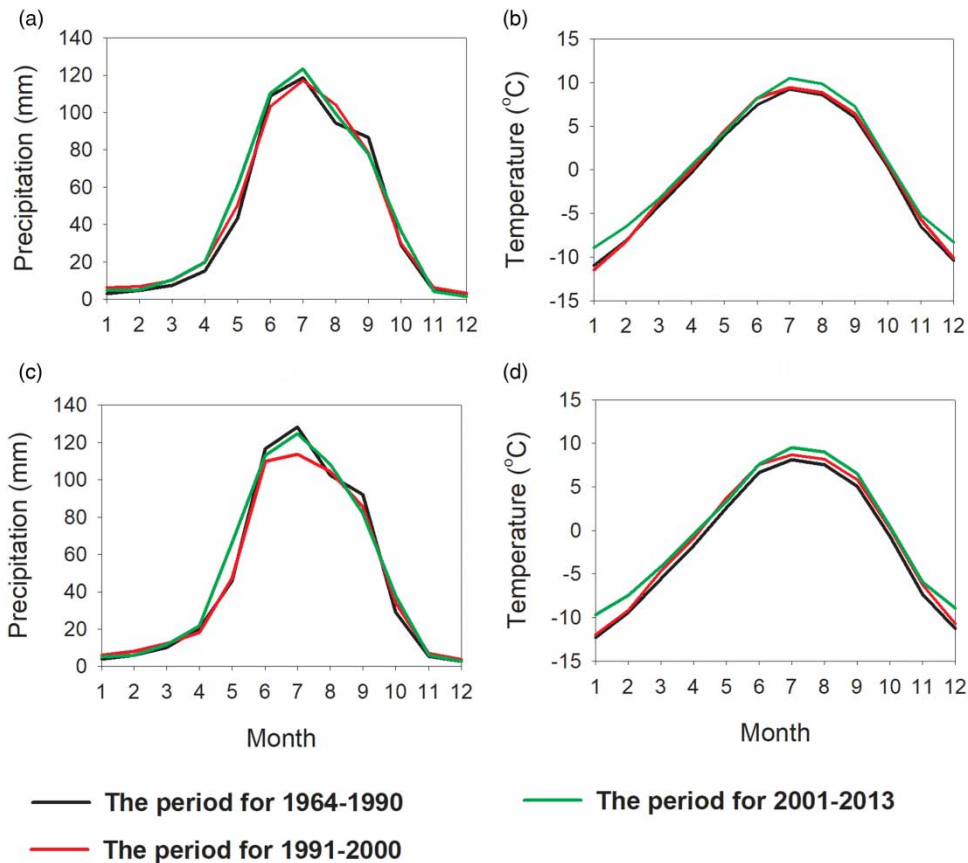


Figure 8 | Mean monthly precipitation and temperature during three periods of 1964–1990, 1991–2000 and 2001–2013: (a) and (b) are results in the UM; (c) and (d) are results in the US.

Table 6 | Trends for simulated runoff components during 1964–2013

Basin	Total runoff	Rainfall runoff	Snowmelt runoff	Glacial runoff
UM	$6.845 \times 10^7 \text{ m}^3/\text{year}^a$	$6.6 \times 10^7 \text{ m}^3/\text{year}^a$	$0.105 \times 10^7 \text{ m}^3/\text{year}$	$0.14 \times 10^7 \text{ m}^3/\text{year}^a$
US	$4.67 \times 10^7 \text{ m}^3/\text{year}$	$3.93 \times 10^7 \text{ m}^3/\text{year}$	$-0.4 \times 10^7 \text{ m}^3/\text{year}$	$1.14 \times 10^7 \text{ m}^3/\text{year}^a$

^aSignificance 0.05.

rainfall runoff exhibits an increment of 4.62% in comparison to 1964–1990.

In respect of snowmelt runoff, the long-term monthly average values in three periods over the focus areas are listed in Figure 9(c) and 9(d). In the UM, the snowmelt runoff peaks in June during 1964–1990 but, nevertheless, the peak shifts from June in the baseline period to May for both the 1990s and 2000s. In the 1990s, compared to that in the baseline period, a relatively large increment in spring is observed while the other months show a little decrease, and thus the annual snowmelt runoff in the UM

suggests an increase of 8.19% relative to the baseline period. In the 2000s, there is also moderate increase during spring but considerable decrease can be noticed among other months and, therefore, the annual snowmelt runoff has been reduced by 5.63%. Meanwhile, for the US, compared to the baseline times, the months for February–April experience a small increase during the 1990s and there is also some growth during February–May in the 2000s, whereas most of the remaining months witness relatively large reductions for both the 1990s and 2000s, and therefore the annual snowmelt runoff indicates a decrease

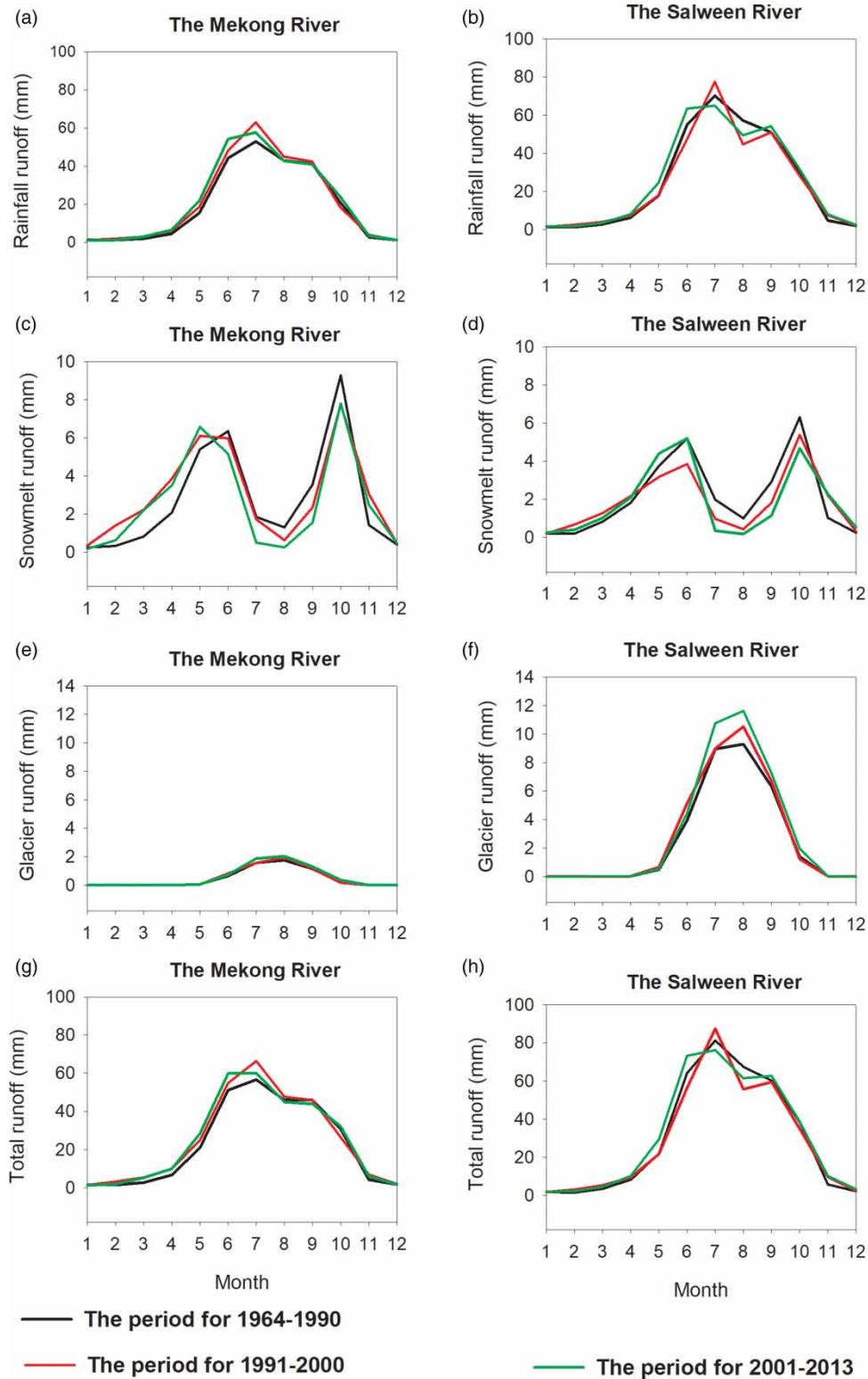


Figure 9 | Mean monthly rainfall runoff, snowmelt runoff, glacier runoff and total runoff in the study regions for three periods of 1964–1990, 1991–2000 and 2001–2013: (a), (c), (e) and (g) are the results in the UM; (b), (d), (f) and (h) are the results in the US.

Table 7 | Proportional contribution for controlling trend of total runoff to three runoff components during 1964–2013

Basin	Trend of total runoff (m ³ /year)	Contribution from rainfall runoff (%)	Contribution from snowmelt runoff (%)	Contribution from glacial runoff (%)
UM	6.845×10^7	96.42	1.54	2.04
US	4.670×10^7	84.22	−8.56	24.33

of 11.55% and 11.14% for the two periods, respectively. As we can see, there is more snowmelt runoff in spring for both the 1990s and 2000s in the UM and for the 2000s in the US, compared to the baseline period. This phenomenon is probably concerned with the increasing precipitation during spring season in the 2000s over these two regions relative to 1964–1990 (Figure 8(a) and 8(c)). Due to the low temperature during spring, part of precipitation falls as snowfall and it melts quickly after a brief stay above the ground with the rise of temperature; its contribution to river runoff is suggested as ‘snowfall runoff’. Therefore, the increasing precipitation may generate more snowfall in spring for the 2000s in both the UM and US, and results in a larger snowmelt runoff during this season relative to that of 1964–1990. Some other researchers also found that during the wet spring season, there is still some snowfall and the following snowmelt runoff over the investigated areas, such as the headwaters of the Yellow River (Cuo *et al.* 2013) and the upstream region of the Yarkant River (Kan *et al.* 2018).

Compared to the variation of rainfall and snowmelt runoff, changes in glacier runoff (Figure 9(e) and 9(f)) exhibit more consistency for the 1990s and 2000s across the two regions relative to 1964–1990. Glacier runoff demonstrates an increasing trend during the melting season (June to September) for both periods compared to that of baseline period. The annual average ice melt increased by about 8.4% and 9.3% for the UM and US in the 1990s in comparison with the reference period. In terms of changes for the 2000s, the glacier runoff indicates a respective increment of 19.3% and 20% in the UM and US relative to 1964–1990.

Due to changes that occurred in rainfall runoff, snowmelt and glacier runoff, the total runoff also underwent a corresponding variation during the 1990s and 2000s

(Figure 9(g) and 9(h)). The variations for the 1990s and 2000s relative to the baseline period are similar to that of rainfall runoff.

The controlling roles of runoff components in the trend of river flow for the past 50 years

Based on the statistical results, both the total runoffs in the UM and US show a rising trend during 1964–2013, with an increment of 6.845×10^7 m³/yr and 4.67×10^7 m³/yr, respectively (Table 6). The individual role of rainfall runoff, snowmelt and glacial runoff in controlling the variation of total runoff can be quantitatively derived according to Equations (10) and (11). Table 7 lists the corresponding controlling roles of each runoff constituent in the trend of runoff for the years 1964–2013.

The roles of rainfall runoff, snowmelt and glacial runoff vary from basin to basin in the tendency of total runoff. For the UM, the increasing total runoff is the compounded effect of the rainfall runoff, snowmelt runoff and glacial runoff, all of which impose a positive impact on the upward trend of total runoff. In terms of respective hydrological role, the rainfall runoff, snowmelt and glacial runoff indicate a particular contribution of 96.42% (6.6×10^7 m³/yr was divided by 6.845×10^7 m³/yr), 1.54% (0.105×10^7 m³/yr was divided by 6.845×10^7 m³/yr) and 2.04% (0.14×10^7 m³/yr was divided by 6.845×10^7 m³/yr) to the change trend of the total runoff for the period of 1964–2013 (Table 7). Meanwhile, for the US, the increasing rainfall runoff (3.93×10^7 m³/yr) and glacial runoff (1.14×10^7 m³/yr) both have a positive effect on the ascending trend of total runoff while decreasing snowmelt runoff (-0.4×10^7 m³/yr) imposes a negative impact on the change of total runoff, and is responsible for 84.22%, 24.33% and −8.56% in order.

DISCUSSION

The hydrological role of melt runoff

In this study, the rainfall runoff contributes to more than 85% of total runoff over the UM and US and so it is the dominant runoff component, which is similar to the study of Lutz *et al.* (2014). Being located in the southeastern

Tibetan Plateau, the two basins are under the impact of the Asia monsoon and receive a large amount of precipitation during summer, and thus the hydrological regime is rain dominated. The runoff regime in other basins of the eastern TP, such as the upstream region of the Yellow River, the Yangtze River, are also mainly controlled by rainfall (Immerzeel *et al.* 2010; Su *et al.* 2016). However, although the melt runoff from glacier and snow cover is limited and no more than 15% of the total runoff over these two regions, it is still playing an important role in both water environment protection and available water resources for the local and further downstream regions. On the one hand, the water quality for the melt runoff is especially good as there is little or negligible pollution over the remote and inaccessible glacier or the snow cover, so the snow and glacial runoff could partly supply high-quality clean water resources to the downstream, and also would neutralize or mitigate the polluted water in the downstream basin. On the other hand, melt water is very important during dry years (the anti-cyclic behaviour) in summer monsoon-dominated areas such as the two focus basins in our study. When anti-cyclic behaviour occurs, the summer precipitation decreases sharply and thus the basins lack sufficient water supply from rainfall. Then, the melt water from glacier and snow cover could compensate for the potential water shortage in the local region and, to some extent, buffer the negative trend of decreasing discharge from the upper region to the downstream basin. This phenomenon is generally referred to as the glacier compensation effect (Zhao *et al.* 2015). As shown in Figure 10, there is an obvious negative correlation between

glacial runoff and river total runoff during the warm season (May–October) over the two basins, which indicates that there is less glacial runoff in wet years but more glacial runoff in dry years. Taking the US as an example (Figure 10(b)), the maximum contribution for glacial runoff to river total runoff can approach 16% during an extreme dry year while the mean value for glacial runoff's contribution is less than 8%. Hence, in these two regions, the regulating capacity for glacial runoff in total runoff is important and cannot be ignored even if the glacier area is no more than 2% of the whole basin.

In the future, the changes in temperature and precipitation will be expected to seriously affect the melt characteristics and the hydrologic regimes over these high-altitude regions, including changes in runoff magnitude, shift of intra-annual patterns of streamflow and the advance of turning point for glacial runoff. Therefore, more detailed study will be dedicated to the analysis of the hydrological effect of climate change in the region.

Model uncertainty

In this study, the VIC model linking with degree-day glacier algorithm, referred to as the VIC-glacier model, was utilized to detect the hydrological regime variation under recent warming climate. Although the VIC-glacier model was calibrated by using observed data or satellite data, there is still some probable uncertainty.

As indicated in Table 7, the glacial runoff plays an important role in controlling streamflow trend over these two basins, although it is not the dominant factor for the

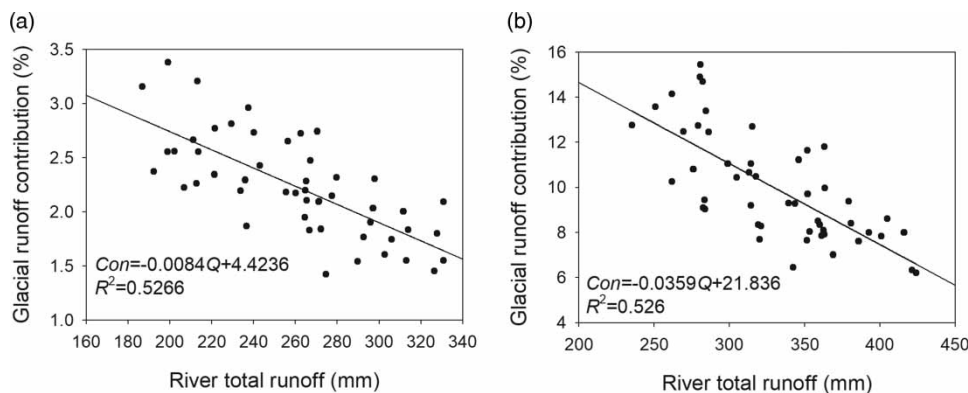


Figure 10 | Scatterplots of glacial runoff contribution (Con) versus river total runoff (Q) during the warm season (May–October) for 1964–2013 in the UM (a) and US (b).

river flow variation. Glacier melt runoff was simulated by the degree-day model and the DDFs are key parameters in this model. In this study, DDF_{ice} and DDF_{snow} were calibrated using glacier change data and observed streamflow data. Also, the mass balance observation on the Xiaodongkemadi glacier is used as auxiliary data for constraining the DDF_{ice} and DDF_{snow} . The final determined values for DDF_{ice} and DDF_{snow} are in the range of these parameters (Table 3). Also, the DDF_{ice} and DDF_{snow} in our study are comparable to other studies in the same regions. For example, the study from Su *et al.* (2016) indicates that their adopted DDF_{ice} for UM and US is $13.8 \text{ mm } ^\circ\text{C}^{-1} \text{ day}^{-1}$ and $7.1 \text{ mm } ^\circ\text{C}^{-1} \text{ day}^{-1}$, respectively, which are comparable to our results. However, the DDFs have large spatial and temporal variation, which could greatly affect the accuracy of snow and ice melt modelling (Hock 2003; Tong *et al.* 2016). Even a single glacier could be subject to significant small-scale variations across its surface (Zhang *et al.* 2006). Meanwhile, altitude is also an important factor affecting the DDFs. Larger DDFs are found on glaciers situated at higher altitude, which may be caused by larger radiation and lower positive degree-day sum at the higher altitude (Kayastha *et al.* 2003). In our work, the two groups of constant DDFs for the UM and US basically represent an average condition for glaciers in the respective basin, and would unavoidably result in uncertainties in the simulation results. Figure 11 exhibits the sensitivity of glacial runoff to the parameters of DDFs in the UM. The mean annual glacier melt runoff would decrease/increase about 10% with the decrease/increase of one unit DDF ($\text{mm } ^\circ\text{C}^{-1} \text{ day}^{-1}$) in

this basin, which is consistent with the findings in the upstream of Yarkant basin in the Karakoram (Kan *et al.* 2018) and the Siling Co basin in the TP (Tong *et al.* 2016). The current glacier scheme (the degree-day model) has a lower complexity than other processes included in the VIC model. The extended degree-day model, in which DDFs account for the effect of aspect in mountain region and also vary with season, corresponding to the spatial and temporal variation, is currently under way to yield more realistic melt estimates and further decrease the uncertainty in the runoff modelling over the TP.

Limited to the scarcity of other data such as measured soil moisture or frozen soil depth, only the observed streamflow data are utilized to calibrate VIC soil and baseflow parameters in hydrological modelling over the ice-free region, which may induce uncertainty in runoff simulation in these areas. In the future, more observed data, including groundwater level and permafrost depth, will be collected to comprehensively calibrate hydrological parameters, and this would increase the robustness of the model and decrease uncertainty during hydrological modelling in the TP basin.

CONCLUSIONS

In this study, a coupled VIC and glacier model was applied to two catchments located in the Tibetan Plateau region to analyse the temporal evolution of the rainfall runoff, snow and glacier melt contribution to river total runoff during the

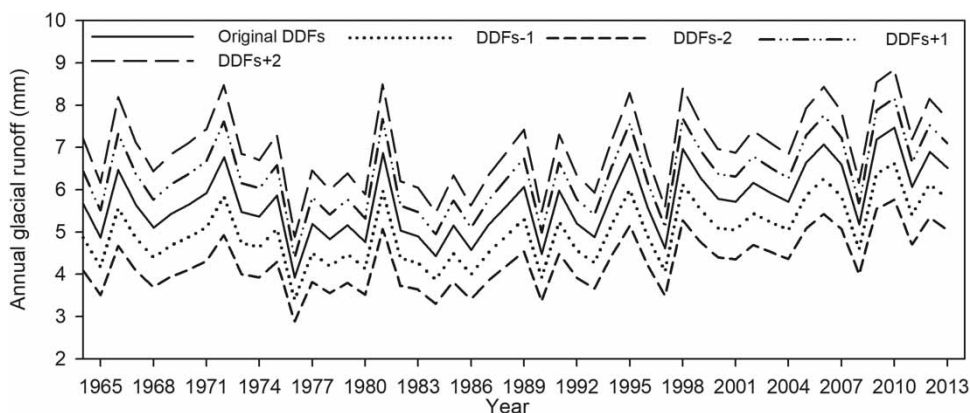


Figure 11 | Simulated annual glacial runoff with different DDFs in the UM for 1964–2013.

past 50 years, and also to evaluate their roles in controlling streamflow trends. The following conclusions were made.

During the past 50 years, the total streamflow indicates an increasing trend in the two focus areas. There is also a general increasing trend for both rainfall runoff and glacial runoff in the UM and US. In terms of snowmelt runoff, it demonstrates an increasing trend over the UM while a decreasing tendency is exhibited in the US.

The rainfall runoff was considered as the dominant factor driving changes of river discharge, which can be responsible for over 84% of changes in the total runoff over all focus catchments. Meanwhile, the glacial runoff illustrates an increasing important role in the controlling streamflow trend under continuous climate warming, in comparison to the snowmelt runoff. Findings from this study can provide beneficial reference to water resource and eco-environment management strategies for governmental policy-makers.

ACKNOWLEDGEMENTS

This work was supported by the National Natural Foundation of China (51379179) and the National key research projects of China (Grant No. 2016YFC0402704). We thank Fengge Su and Leilei Zhang for their help in the VIC data preparation over our studies areas. We also appreciate the editor and two anonymous reviewers for their constructive comments.

REFERENCES

- Barnett, T. P., Adam, J. C. & Lettenmaier, D. P. 2005 Potential impacts of a warming climate on water availability in snow-dominated regions. *Nature* **438** (7066), 303–309.
- Bolch, T., Kulkarni, A., Kaab, A., Huggel, C., Paul, F. & Cogley, J. G. 2012 The state and fate of Himalayan glaciers. *Science* **336** (6079), 310–314.
- Cao, J., Qin, D., Kang, E. & Li, Y. 2006 River discharge changes in the Qinghai-Tibet Plateau. *Chinese Science Bulletin* **51** (5), 594–600.
- Chen, X., Long, D., Hong, Y., Zeng, C. & Yan, D. 2017 Improved modeling of snow and glacier melting by a progressive two-stage calibration strategy with GRACE and multisource data: how snow and glacier meltwater contributes to the runoff of the Upper Brahmaputra River basin? *Water Resources Research* **53** (3), 2431–2466.
- Cuo, L., Zhang, Y., Gao, Y., Hao, Z. & Cairang, L. 2013 The impacts of climate change and land cover/use transition on the hydrology in the upper Yellow River Basin, China. *Journal of Hydrology* **502**, 37–52.
- Duan, A. & Wu, G. 2006 Change of cloud amount and the climate warming on the Tibetan Plateau. *Geophysical Research Letters* **33**, 22.
- FAO – UNESCO 1988 *UNESCO Soil Map of the World, Revised Legend*. World Resources Report 60. FAO, Rome, Italy.
- Feng, S., Hu, Q. & Qian, W. 2004 Quality control of daily meteorological data in China, 1951–2000: a new dataset. *International Journal of Climatology* **24** (7), 853–870.
- Hock, R. 2003 Temperature index melt modelling in mountain areas. *Journal of Hydrology* **282** (1), 104–115.
- Immerzeel, W. W., Droogers, P., De Jong, S. & Bierkens, M. 2009 Large-scale monitoring of snow cover and runoff simulation in Himalayan river basins using remote sensing. *Remote Sensing of Environment* **113** (1), 40–49.
- Immerzeel, W. W., Van Beek, L. P. & Bierkens, M. F. 2010 Climate change will affect the Asian water towers. *Science* **328** (5984), 1382–1385.
- Jacob, T., Wahr, J., Pfeffer, W. T. & Swenson, S. 2012 Recent contributions of glaciers and ice caps to sea level rise. *Nature* **482** (7386), 514.
- Kan, B., Su, F., Xu, B., Xie, Y., Li, J. & Zhang, H. 2018 Generation of high mountain precipitation and temperature data for a quantitative assessment of flow regime in the Upper Yarkant Basin in the Karakoram. *Journal of Geophysical Research: Atmospheres* **123** (16), 8462–8486.
- Kaser, G., Großhauser, M. & Marzeion, B. 2010 Contribution potential of glaciers to water availability in different climate regimes. *Proceedings of the National Academy of Sciences* **107** (47), 20223–20227.
- Kayastha, R., Ageta, Y., Nakawo, M., Fujita, K., Sakai, A. & Matsuda, Y. 2003 Positive degree-day factors for ice ablation on four glaciers in the Nepalese Himalaya and Qinghai-Tibetan Plateau. *Bulletin of Glaciological Research* **20**, 7–14.
- Kendall, M. 1975 *Rank Correlation Methods*. Griffin & Co, London, UK. ISBN 0-85264-199-0.
- Kimball, J., Running, S. & Nemani, R. 1997 An improved method for estimating surface humidity from daily minimum temperature. *Agricultural and Forest Meteorology* **85** (1), 87–98.
- Kotlyakov, V., Zichu, X., Khromova, T., Zverkova, N. & Chernova, L. 2012 Contemporary glacier systems of continental Eurasia. *Doklady Earth Sciences* **446**, 1095–1098.
- Kuang, X. & Jiao, J. J. 2016 Review on climate change on the Tibetan Plateau during the last half century. *Journal of Geophysical Research: Atmospheres* **121**, 8.
- Kumar, S., Merwade, V., Kam, J. & Thurner, K. 2009 Streamflow trends in Indiana: effects of long term persistence, precipitation and subsurface drains. *Journal of Hydrology* **374** (1), 171–183.

- Li, C., Su, F., Yang, D., Tong, K., Meng, F. & Kan, B. 2018 Spatiotemporal variation of snow cover over the Tibetan Plateau based on MODIS snow product, 2001–2014. *International Journal of Climatology* **38** (2), 708–728.
- Liang, X., Lettenmaier, D. P., Wood, E. F. & Burges, S. J. 1994 A simple hydrologically based model of land surface water and energy fluxes for general circulation models. *Journal of Geophysical Research* **99** (D7), 14415–14428.
- Liang, X., Wood, E. F. & Lettenmaier, D. P. 1996 Surface soil moisture parameterization of the VIC-2 L model: evaluation and modification. *Global and Planetary Change* **13** (1), 195–206.
- Liu, W., Sun, F., Li, Y. & Zhang, G. 2018a Investigating water budget dynamics in 18 river basins across the Tibetan Plateau through multiple datasets. *Hydrology & Earth System Sciences* **22**, 1–56.
- Liu, Z., Wang, R. & Yao, Z. 2018b Climate change and its impact on water availability of large international rivers over the mainland Southeast Asia. *Hydrological Processes* **32** (26), 3966–3977.
- Lu, M., Yang, S., Li, Z., He, B., He, S. & Wang, Z. 2017 Possible effect of the Tibetan Plateau on the ‘upstream’ climate over West Asia, North Africa, South Europe and the North Atlantic. *Climate Dynamics* **6**, 1–14.
- Lutz, A., Immerzeel, W., Shrestha, A. & Bierkens, M. 2014 Consistent increase in High Asia’s runoff due to increasing glacier melt and precipitation. *Nature Climate Change* **4** (7), 587–592.
- Ma, Y., Zhong, L., Su, Z., Ishikawa, H., Menenti, M. & Koike, T. 2006 Determination of regional distributions and seasonal variations of land surface heat fluxes from Landsat-7 Enhanced Thematic Mapper data over the central Tibetan Plateau area. *Journal of Geophysical Research: Atmospheres* **111**, D10305.
- Mann, H. B. 1945 Nonparametric tests against trend. *Econometrica: Journal of the Econometric Society* **13** (3), 245–259.
- Meng, F., Su, F., Li, Y. & Tong, K. 2019 Changes in terrestrial water storage during 2003–2014 and possible causes in Tibetan Plateau. *Journal of Geophysical Research: Atmospheres* **124**, 2909–2931.
- Pu, Z., Xu, L. & Salomonson, V. V. 2007 Modis/terra observed seasonal variations of snow cover over the Tibetan Plateau. *Geophysical Research Letters* **34** (6), L06706.
- Qiu, J. 2008 China: the third pole. *Nature News* **454** (7203), 393–396.
- Shen, Y. & Xiong, A. 2016 Validation and comparison of a new gauge-based precipitation analysis over mainland China. *International Journal of Climatology* **36** (1), 252–265.
- Shen, Y. J., Shen, Y., Fink, M., Kralisch, S. & Brenning, A. 2018 Unraveling the Hydrology of the glacierized Kaidu Basin by integrating multisource data in the Tianshan Mountains, Northwestern China. *Water Resources Research* **54**, 557–580.
- Su, F., Adam, J. C., Bowling, L. C. & Lettenmaier, D. P. 2005 Streamflow simulations of the terrestrial Arctic domain. *Journal of Geophysical Research: Atmospheres* **110**, D8.
- Su, F., Zhang, L., Qu, T., Chen, D., Yao, T., Tong, K. & Qi, Y. 2016 Hydrological response to future climate changes for the major upstream river basins in the Tibetan Plateau. *Global Planet Change* **136**, 82–95.
- Tong, K., Su, F. & Xu, B. 2016 Quantifying the contribution of glacier-melt water in the expansion of the largest lake in Tibet. *Journal of Geophysical Research: Atmospheres* **121**, 11158–11173.
- Wang, S. J. 2017 Spatiotemporal variability of temperature trends on the southeast Tibetan Plateau, China. *International Journal of Climatology* **38** (5), 1953–1963.
- Wang, H. & Chen, F. 2017 Increased stream flow in the Nu River (Salween) Basin of China, due to climatic warming and increased precipitation. *Geografiska Annaler: Series A, Physical Geography* **99** (4), 327–337.
- Wu, Y. H., Zheng, H. X., Zhang, B., Chen, D. M. & Lei, L. P. 2014 Long-term changes of lake level and water budget in the Nam Co Lake Basin, central Tibetan Plateau. *Journal of Hydrometeorology* **15** (3), 1312–1322.
- Yao, T., Wang, Y., Liu, S., Pu, J., Shen, Y. & Lu, A. 2004 Recent glacial retreat in High Asia in China and its impact on water resource in Northwest China. *Science in China Series D: Earth Sciences* **47** (12), 1065–1075.
- Yao, T., Thompson, L. & Yang, W. 2012 Different glacier status with atmospheric circulations in Tibetan Plateau and surroundings. *Nature Climate Change* **2** (9), 663–667.
- Yao, Z., Liu, Z., Huang, H., Liu, G. & Wu, S. 2014 Statistical estimation of the impacts of glaciers and climate change on river runoff in the headwaters of the Yangtze River. *Quaternary International* **336**, 89–97.
- Zhang, Y., Liu, S. & Ding, Y. 2006 Observed degree-day factors and their spatial variation on glaciers in western China. *Annals of Glaciology* **43** (1), 301–306.
- Zhang, Y., Liu, S., Xu, J. & Shangguan, D. 2008 Glacier change and glacier runoff variation in the Tuotuo River basin, the source region of Yangtze River in western China. *Environmental Geology* **56** (1), 59–68.
- Zhang, L., Su, F., Yang, D., Hao, Z. & Tong, K. 2013 Discharge regime and simulation for the upstream of major rivers over Tibetan Plateau. *Journal of Geophysical Research: Atmospheres* **118** (15), 8500–8518.
- Zhao, Q., Zhang, S., Ding, Y. J., Wang, J., Han, H. & Xu, J. 2015 Modeling hydrologic response to climate change and shrinking glaciers in the highly glacierized kunma like river catchment, central Tian Shan. *Journal of Hydrometeorology* **16** (6), 2383–2402.

First received 30 May 2019; accepted in revised form 8 September 2019. Available online 10 October 2019